Liquid Crystals
Publication details, including instructions for authors and subscription information:
http://www.informaworld.com/smpp/title~content=t713926090

Anchoring Properties of Nematic Liquid Crystals Studied Using the Attenuated Total Reflection Method

Li Chang[a]; Jing-An Zhao[a]; Xin-Jiu Wang[a]
[a] Liquid Crystal Research Group, Department of Physics, Tsinghua University, Beijing, China

To cite this Article Chang, Li , Zhao, Jing-An and Wang, Xin-Jiu(1987) 'Anchoring Properties of Nematic Liquid Crystals Studied Using the Attenuated Total Reflection Method', Liquid Crystals, 2: 3, 251 — 260
To link to this Article: DOI: 10.1080/02678298708086674
URL: http://dx.doi.org/10.1080/02678298708086674

LIQUID CRYSTALS, 1987, VOL. 2, No. 3, 251–260

Anchoring properties of nematic liquid crystals studied using the attenuated total reflection method

by LI CHANG, JING-AN ZHAO and XIN-JIU WANG
Liquid Crystal Research Group, Department of Physics, Tsinghua University, Beijing, China

(*Received 14 May 1986; accepted 1 November 1986*)

By using the attenuated total reflection method associated with the excitation of surface plasmons, the tilt angle of the liquid crystal director and its gradient at the surface are measured in a planar nematic cell as a function of the applied voltage. The surface anchoring anisotropy $\Delta\pi$ of the liquid crystal and the surface elastic constant k_s are found to be $\Delta\pi = 0{\cdot}288$ erg/cm and $k_s = 9{\cdot}12 \times 10^{-11}$ erg, respectively, when the boundary condition suggested by Barbero *et al.* is used. The theoretical and experimental values obtained with this boundary condition and that of Mada are discussed. The results show that the boundary condition proposed by Barbero *et al.* is in better agreement with the experiment.

1. Introduction

Liquid crystal display devices have to be surface aligned for good performance. Surface alignment in a liquid crystal cell is also necessary for the measurement of the material parameters such as the refractive indices, permittivities, elastic constants, etc. But the mechanism of the director alignment at the substrate is not well understood. Several theories and experimental methods [1–3] have been developed in recent years; the attenuated total reflection (ATR) method is one of the most useful [2].

Initially the tilt angle of the director at the surface was considered to be unaffected by the applied field; this is called the strong anchoring limit. This assumption was used to calculate the threshold field of liquid crystal devices [4, 5]. Later on, it was found [1] that the director at the substrate does change with the applied field, i.e. weak boundary coupling is closer to the truth. The anchoring energy is found to have a cosine square (or sine square) dependence on the orientation angle at the substrate. The dependence of the director angle on the applied field was analysed by Nehring *et al.* [6] assuming equal elastic constants. Subsequently, the dependence of the surface tilt angle and its gradient on the applied voltage was measured by Sprokel *et al.* [7] using the ATR method. A thin layer of silicon dioxide (SiO_2) was evaporated on the substrate to align the director. It was found that there is significant difference between the experimental results and the theoretical prediction based on the strong anchoring assumption. Subsequently, Yang [8] and Mada [9] pointed out that the theoretical values from the weak boundary coupling assumption are in good agreement with the experiment of Sprokel *et al.*

In this paper, liquid crystal anchoring on the substrate SiO is studied by the ATR method. Our experimental results are then analysed with the phenomenological theory [10, 11] together with the boundary conditions proposed by Barbero *et al.* [11] and Mada [10].

2. Theory

In an aligned liquid crystal cell of thickness d, the z axis is taken to be perpendicular to the substrate (shown in figure 1 (*b*)). A general form of the surface free energy of the nematic liquid crystal is given by [10, 11]

$$\Lambda = \Lambda_d + \Lambda_e, \tag{1}$$

where Λ_d is the surface deformation energy per unit area and Λ_e is the energy related to the easy axis. In the planar cell case (used in our experiments) Λ_d takes the form

$$\Lambda_d = \tfrac{1}{2} k_s \sin^2 \theta_b \cos^2 \theta_b \, (d\theta/dz)_b^2, \tag{2}$$

where k_s is the surface elastic constant, θ_b and $(d\theta/dz)_b$ are respectively the tilt angle of the director with respect to the x axis and its gradient evaluated at the surface $z = 0$ or $z = d$. Λ_e is defined by

$$\Lambda_e = -\tfrac{1}{2}\Delta\pi(\sin^2\theta_b - \tfrac{1}{3}), \tag{3 a}$$

or

$$\Lambda_e = -\tfrac{1}{2}\Delta\pi(\cos^2\theta_b - \tfrac{1}{3}). \tag{3 b}$$

Equations (3 *a*) and (3 *b*) correspond to the easy axis being perpendicular and parallel to the surface, respectively. $\Delta\pi$ is the surface anchoring anisotropy, corresponding to the orienting action of the cell; the total free energy per unit area is given by

$$F = \int_0^d \Lambda_b \, dz + \Lambda(z = 0) + \Lambda(z = d), \tag{4}$$

where Λ_b is the bulk free energy density given by

$$\Delta_b = \tfrac{1}{2}(k_{11}\cos^2\theta + k_{33}\sin^2\theta)(d\theta/dz)^2 + \frac{D^2}{2\varepsilon_\perp(1 + \varepsilon\sin^2\theta)} + \tfrac{1}{2}k_{13}\frac{d}{dz}\left(\sin 2\theta \frac{d\theta}{dz}\right). \tag{5}$$

Here θ is the angle between the director and the x axis, and is a function of z, k_{11} and k_{33} are the splay and bend elastic constants, respectively, $\varepsilon = (\varepsilon_\parallel - \varepsilon_\perp)/\varepsilon_\perp$; $\varepsilon_\parallel$

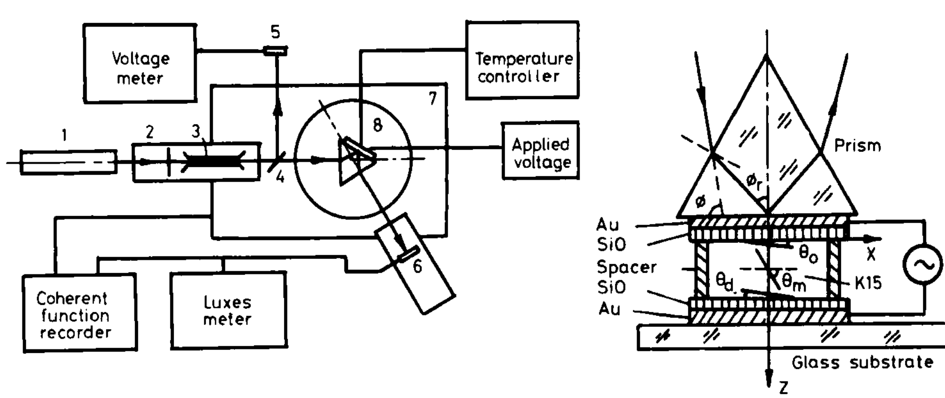

Figure 1. (*a*) Sketch of the experimental set-up; 1, He–Ne laser; 2, polarizer; 3, collimator; 4, splitter; 5, electric cell; 6, light receiver; 7, ϕ–2ϕ rotator; 8, sample. (*b*) Liquid crystal cell, ϕ is the measured angle.

and $\varepsilon_{\perp}$ are the permittivities parallel and perpendicular to the director, respectively, D the dielectric displacement. k_{13} is discussed by Nehring and Saupe [12] but following [13], we neglect the influence of the k_{13} term. The Euler–Lagrange equation corresponding to the stable configuration of the director can be obtained as

$$\frac{\partial \Lambda_b}{\partial \theta} - \frac{d}{dz}\left[\frac{\partial \Lambda_b}{\partial(d\theta/dz)}\right] = 0. \tag{6}$$

The boundary condition proposed by Barbero *et al.* is [11]

$$-\left[\frac{\partial \Lambda_b}{\partial(d\theta/dz)}\right]_0 + \frac{\partial \Lambda}{\partial \theta_0} + \left[\frac{\partial \Lambda(z=0)}{\partial(d\theta/dz)}\frac{\partial(d\theta/dz)}{\partial \theta_0}\right]_0 + \left[\frac{\partial \Lambda(z=d)}{\partial(d\theta/dz)}\frac{\partial(d\theta/dz)}{\partial \theta_0}\right]_d = 0$$

and

$$\left[\frac{\partial \Lambda_b}{\partial(d\theta/dz)}\right]_d + \frac{\partial \Lambda}{\partial \theta_d} + \left[\frac{\partial \Lambda(z=d)}{\partial(d\theta/dz)}\frac{\partial(d\theta/dz)}{\partial \theta_d}\right]_d + \left[\frac{\partial \Lambda(z=0)}{\partial(d\theta/dz)}\frac{\partial(d\theta/dz)}{\partial \theta_d}\right]_0 = 0, \tag{7}$$

the subscripts 0 and d represent the values at the two surfaces at $z = 0$ and $z = d$, respectively.

From equation (6), after trivial calculation, we obtain

$$\frac{d\theta}{dz} = \frac{2}{d}\left[\frac{\sin^2\theta_m - \sin^2\theta}{(1 - k\sin^2\theta)(1 + \varepsilon\sin^2\theta)}\right]^{1/2}\int_{\theta_0}^{\theta_m}\left[\frac{(1 - k\sin^2\theta)(1 + \varepsilon\sin^2\theta)}{\sin^2\theta_m - \sin^2\theta}\right]^{1/2} d\theta, \tag{8}$$

where θ_m is the tilt angle at $z = d/2$ (see figure 1 (*b*), and $k = (k_{11} - k_{33})/k_{11}$. For an applied voltage V, the maximum deformation angle θ_m is given implicitly by

$$\begin{aligned} V &= 2\int_0^{d/2} E\,dz, \\ &= 2\left[\frac{k_{11}(1 + \varepsilon\sin^2\theta_m)}{\varepsilon_{\perp}\varepsilon}\right]^{1/2}\int_{\theta_0}^{\theta_m}\left[\frac{1 - k\sin^2\theta}{(1 + \varepsilon\sin^2\theta)(\sin^2\theta_m - \sin^2\theta)}\right]^{1/2} d\theta, \end{aligned} \tag{9}$$

where E is the effective electric field inside the liquid crystal cell.

In general, the two substrates ($z = 0$ and $z = d$) may have different anchoring energies. For simplicity, we limit ourselves to a symmetric problem, i.e. $(\Delta\pi)_0 = (\Delta\pi)_d$, $(k_s)_0 = (k_s)_d$, which implies $\theta_0 = \theta_d$, $(d\theta/dz)_0 = -(d\theta/dz)_d$. Substituting equations (1), (2), (3) and (5) into the boundary condition (7), we have

$$\frac{k_{11}(1 - k\sin^2\theta_0)}{\sin\theta_0\cos\theta_0}\left(\frac{d\theta}{dz}\right)_0 - k_s\left[\cos 2\theta_0\left(\frac{d\theta}{dz}\right)_0^2 + \sin 2\theta_0\left(\frac{d\theta}{dz}\right)_0\frac{\partial(d\theta/dz)_0}{\partial\theta_0}\right] \pm \Delta\pi = 0, \tag{10}$$

where the + and − signs in front of $\Delta\pi$ correspond to the easy axis perpendicular or parallel to the substrate, respectively.

3. Experiment and results

The experimental set-up is illustrated in figure 1 (*a*). We have used SiO as an alignment layer and obtained a planar liquid crystal cell with the director parallel to the x axis. A polarized He–Ne laser with $\lambda = 6328$ Å was used. The plane of polarization (p polarized) is in the xz plane and the director is also in this plane. The prism, with all angles equal to $60° \pm 1'$, is made of ZF-7 Glass (produced in China) with a refractive index $n_0 = 1{\cdot}799$. The collimated laser beam with the incident angle ϕ was reflected at the bottom of the prism and the reflected light is received by a Luxes meter synchronously with a $\phi - 2\phi$ rotator. The reflectivity was corrected for the change of laser intensity by an electric cell. The temperature of the liquid crystal cell was controlled at $29 \pm 0{\cdot}5$°C.

The optical system consists of a prism, a thin evaporated gold film, a thin SiO layer and a liquid crystal cell. Its reflectivity is determined by its optical parameters. The numerical model of Sprokel *et al.* [7] was used assuming the nematic adjacent to the substrate to be stratified media of 30 layers each of which is 100 Å in thickness. The values of $n_e(z)$ and $n_0(z)$, the extraordinary and ordinary refractive indices along the z axis, respectively, are assumed to be uniform within each 100 Å layer and are determined from the director orientation in the middle of that layer. The model also assumes that the gradient of the nematic tilt angle is constant and designated as $(d\theta/dz)_0$ for the first 3000 Å near the substrate. From the Fresnel formula the reflectivity was found [14] to be

$$R = (M_{21}/M_{11})^2, \tag{11}$$

where M_{21} and M_{11} are matrix elements of 2×2 matrix $\mathbf{M}$ given by

$$\mathbf{M} = \prod_{n=0}^{n=N} \mathbf{m}_n.$$

Here N is the number of layers and

$$m_n = \begin{bmatrix} \dfrac{U_n + U_{n+1}}{2U_n} \exp(ik_{nz}d_n), & \dfrac{U_n - U_{n+1}}{2U_n} \exp(ik_{nz}d_n) \\ \dfrac{U_n - U_{n+1}}{2U_n} \exp(-ik_{nz}d_n), & \dfrac{U_n + U_{n+1}}{2U_n} \exp(-ik_{nz}d_n) \end{bmatrix}, \tag{12}$$

where d_n is the thickness of the nth layer, and $d_0 = 0$, k_{nz} is the normal component of the wavevector in the nth layer. For a layer of isotropic material, for example, Au and SiO,

$$\left.\begin{aligned} k_{nz} &= -(\varepsilon_n(2\pi/\lambda)^2 - k_{0x}^2)^{1/2}, \\ U_n &= \varepsilon_n/k_{nz}, \end{aligned}\right\} \tag{13}$$

where ε_n is electric permittivity of nth layer. For an anisotropic nematic layer

$$\left.\begin{aligned} k_{nz} &= -k_{0x}\frac{\varepsilon_{xz}}{\varepsilon_{zz}}\frac{(\varepsilon_\parallel\varepsilon_\perp)^{1/2}}{\varepsilon_{zz}}(\varepsilon_{zz}(2\pi/\lambda)^2 - k_{0x}^2)^{1/2}, \\ U_n &= -\left[\frac{\varepsilon_\parallel\varepsilon_\perp}{\varepsilon_{zz}(2\pi/\lambda)^2 - k_{0x}^2}\right]^{1/2}, \\ k_{0x} &= (2\pi/\lambda)n_0 \sin\phi_r, \end{aligned}\right\} \tag{14}$$

where ϕ_r is the reflective angle, which is given by

$$\phi_r = \pi/3 - \sin^{-1}(\sin(\phi - \pi/6)/n_0). \tag{15}$$

Here n_0 is the refractive index of the prism, ε_{xz} and ε_{zz} are functions of the tilt angle of the director of that layer given by

$$\left.\begin{aligned}\varepsilon_{xz} &= (\varepsilon_{\parallel} - \varepsilon_{\perp}) \sin\theta_n \cos\theta_n, \\ \varepsilon_{zz} &= \varepsilon_{\parallel} \sin^2\theta_n + \varepsilon_{\perp} \cos^2\theta_n.\end{aligned}\right\} \qquad (16)$$

Fitting the experimental ATR curves by a non-linear least squares fitting method with respect to ϕ by equations (11)–(16), we can find the optical parameters of the system, such as ε, d and n. When the reflectivity was calculated, R must be corrected for the transmission and reflection at the surface of the prism. These corrections were included in the computer program.

We started with the prism/Au/air system. The dielectric constant ε_1 and film thickness d_1 of gold was found to be

$$\varepsilon_1 = -12{\cdot}56 + i1{\cdot}35, \quad d_1 = 448\,\text{Å}.$$

The SiO layer was then coated. Similarly, the reflective index n_2 and the thickness d_2 of the SiO layer were obtained as

$$n_2 = 1{\cdot}917 \quad \text{and} \quad d_2 = 64{\cdot}6\,\text{Å}.$$

We note that the value of the refractive index n_2 of SiO is nearly in the range 1·95–2·15 as given in [15].

The liquid crystal cell is about 50 μm thick; this cell was filled with nematic K15 (from BDH Chemicals Limited). Similarly, we have also obtained the extraordinary and ordinary refractive indices n_e and n_o when the applied field is absent. They were found to be

$$n_e = 1{\cdot}714 \quad \text{and} \quad n_o = 1{\cdot}484.$$

The values are slightly different from the data published by BDH Chemicals Limited [16], which are

$$n_e = 1{\cdot}702 \quad \text{and} \quad n_o = 1{\cdot}539$$

at 29°C, and for $\lambda = 5890$ Å.

The experimental results and theoretical ATR curves for the three systems, i.e. prism/Au/air, prism/Au/SiO/air and prism/Au/SiO/K15 are shown in figures 2, 3 and 4 (*a*), respectively.

Subsequently, a voltage greater than the threshold voltage was applied across the cell and the director was distorted from its quiescent orientation. Because the anchoring energy is finite, the angle θ_0 made by the director at the substrate is no longer zero, and R is only a function of θ_0. Using equations (8), (9) and (11)–(16), we can determine θ_m, θ_0 and $(d\theta/dz)_0$. The following constants [16] were used in the calculation for the nematic K15:

$$k_{11} = 1{\cdot}34 \times 10^{-7}\,\text{dyn}, \quad k_{33} = 1{\cdot}9 \times 10^{-7}\,\text{dyn},$$

$$\varepsilon_{\parallel} = 17{\cdot}9, \qquad \varepsilon_{\perp} = 6{\cdot}9,$$

These data were obtained at 26°C but they are not that much different from those at 29°C, the temperature for our experiment, because 29°C is far from the nematic–isotropic transition temperature of 35·5°C.

A planar cell implies that the easy axis lies on the substrate and is parallel to the x axis, so the $-$ sign in equation (10) is chosen, and a linear equation was obtained

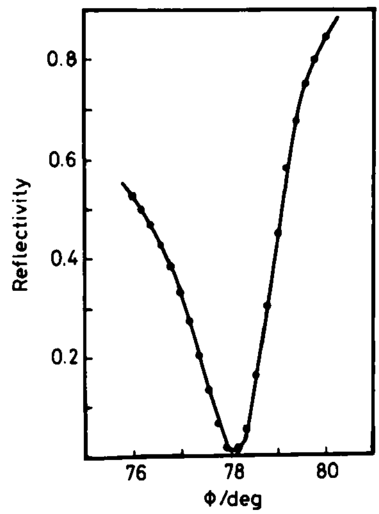

Figure 2. ATR curve for the system prism/Au/air; full circles are the experimental data.

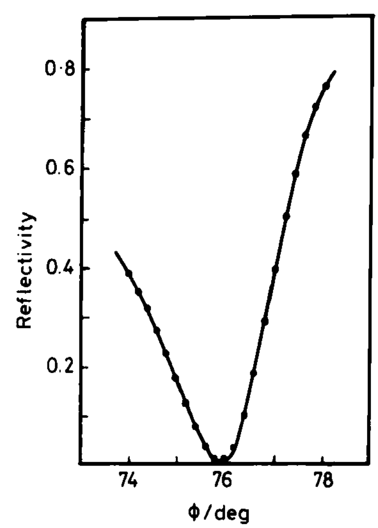

Figure 3. ATR curve for the system prism/Au/SiO/air; full circles are the experimental data.

from equation (10)

$$Y = k_s X + \Delta\pi, \tag{17}$$

where X and Y are functions of θ_m, θ_0 and $(d\theta/dz)_0$ and are therefore a function of the applied voltage V.

For different applied voltages we obtained a series of pairs of (X, Y) points. When Y is plotted against X, according to equation (17), it should be a straight line with slope k_s and an ordinate intercept $\Delta\pi$. Using a linear least square fit, the values of $\Delta\pi$ and k_s were found to be

$$\left.\begin{aligned} \Delta\pi &= 0{\cdot}288\,\mathrm{erg/cm}, \\ k_s &= 9{\cdot}12 \times 10^{-11}\,\mathrm{erg}, \end{aligned}\right\} \tag{18}$$

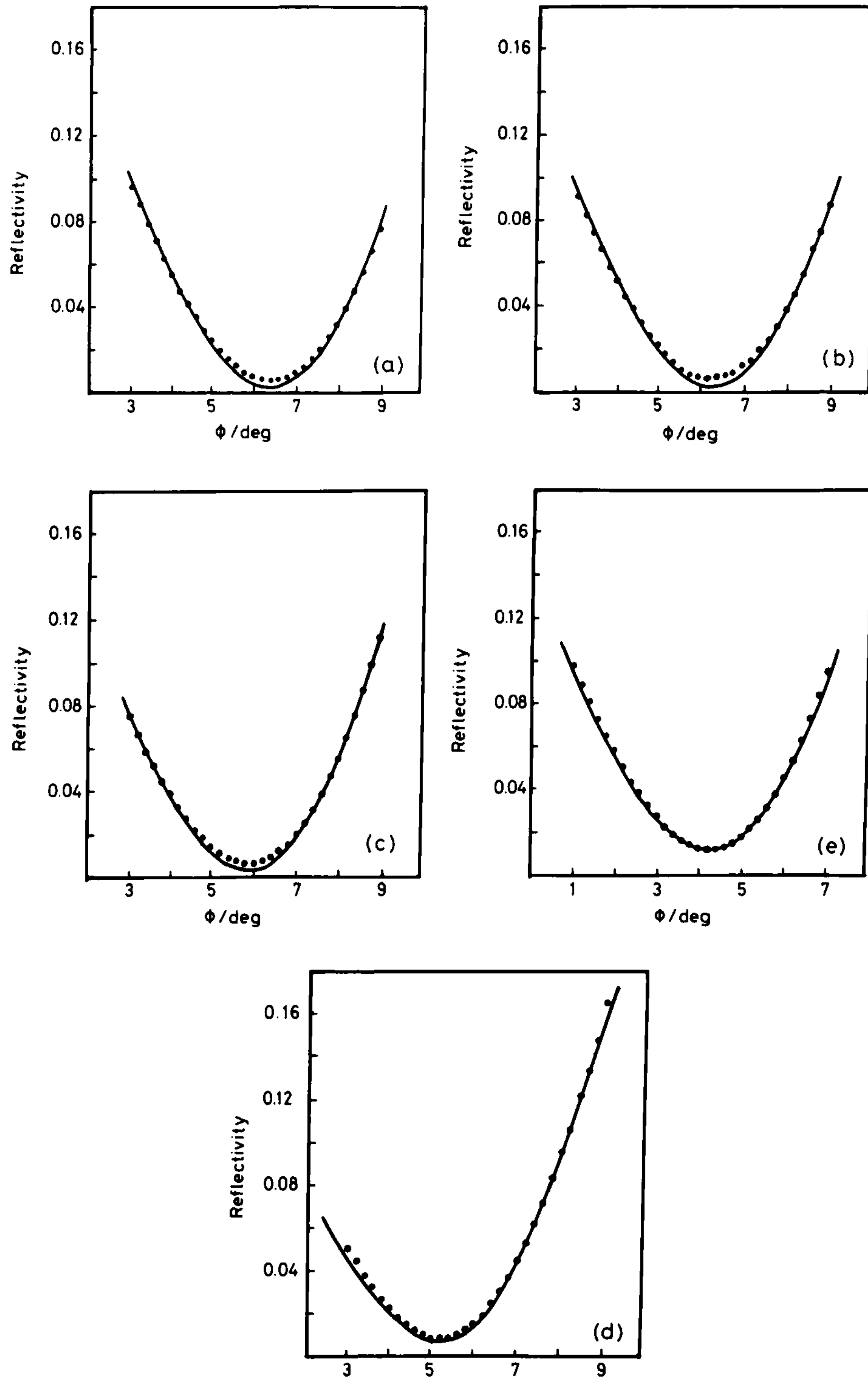

Figure 4. ATR curves but for the system prism/Au/SiO/K15, full circles are the experimental data; (*a*) without an applied voltage; with an applied voltage of (*b*) 2 V; (*c*) 4 V; (*d*) 6 V; (*e*) 8 V.

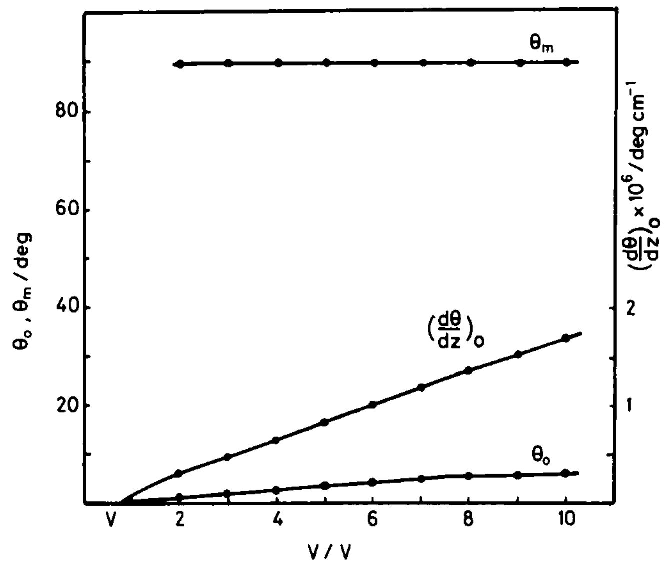

Figure 5. The tilt angle θ_0 of the nematic director, its gradient at the substrate and the maximum deformation angle θ_m versus the applied voltage, V.

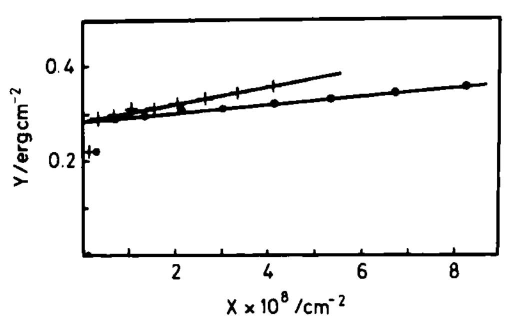

Figure 6. The dependence of equation (17) in the text; full circles are the experimental data from the boundary condition proposed by Barbero *et al.*; crosses are those from the Mada boundary condition.

The dependence of θ_m, θ_0 and $(d\theta/dz)_0$ on V is shown in figure 5. The curve of equation (17) is shown in figure 6. Both the theoretical ATR curves and the experimental data are plotted in figure 4 for comparison. We can see in figure 6 that the boundary condition given in equation (10) represents the alignment of the nematic on the substrate quite well, especially when the applied voltage is high.

4. Discussion and conclusion

Mada [10, 11] used the following boundary condition:

$$-\left[\frac{\partial \Lambda_b}{\partial(d\theta/dz)}\right]_0 + \frac{\partial \Lambda}{\partial \theta_0} - \frac{d}{dz}\left[\frac{\partial \Lambda}{\partial(d\theta/dz)}\right]_0 = 0; \tag{19}$$

this is not the same as equation (7). From equations (1)–(5) and (19), we obtain, after trivial calculation,

$$\frac{k_{11}(1 - k\sin^2\theta_0)}{\sin\theta_0\cos\theta_0}\left(\frac{d\theta}{dz}\right)_0 + \frac{k_s}{2}\left\{\cos 2\theta_0 + \tfrac{1}{4}\sin^2 2\theta_0\left[\frac{k}{1 - k\sin^2\theta_0}\right.\right.$$

$$\left.\left. - \frac{1 + \varepsilon\sin^2\theta_m}{(1 + \varepsilon\sin^2\theta_0)(\sin^2\theta_m - \sin^2\theta_0)}\right]\right\}\left(\frac{d\theta}{dz}\right)_0^2 - \Delta\pi = 0. \quad (20)$$

It can be seen that the term of k_s in equation (20) is different from that in equation (10). By the same procedure, as in § 3 except that equation (10) is replaced by equation (20), we obtain, from our experimental data,

$$\left.\begin{aligned} \Delta\pi &= 0{\cdot}288\,\text{erg/cm}, \\ k_s &= -1{\cdot}74 \times 10^{-10}\,\text{erg}. \end{aligned}\right\} \quad (21)$$

$\Delta\pi$ is exactly the same as the value from the boundary condition proposed by Barbero *et al.* [11], which can obviously be seen in equation (20), but k_s is now negative. Note that Mada's boundary condition in equation (20) does not satisfy $\delta F/\delta\theta = 0$. This has been discussed in detail by Barbero *et al.* [11]; obviously, a negative k_s is unphysical.

The surface elastic constant k_s is determined here for the first time. The value of the surface anchoring anisotropy $\Delta\pi$ in our experiment shows that the SiO alignment layer gives a relatively strong anchoring, which is qualitatively in agreement with previous conclusions [3]. Our result for $\Delta\pi$ is of the same order of magnitude as those in [3, 8, 9].

Until now, the k_s term has been neglected by others [1, 3, 8, 13, 17] in analysing the surface anchoring. As demonstrated in figure 6, the values of the three terms in equation (10), i.e. Y, $k_s X$ and $\Delta\pi$ are of the same order of magnitude. In other words, the energy of surface deformation plays as important a role as the influence of the director deformation in the bulk and as the energy of the easy axis field. The orientation of the director in the liquid crystal cell is determined from the balance of these three terms. If any one of them (e.g. Λ_d) is neglected serious error may be introduced [8].

We thank Chen Hao-ming for assistance in the experiments and Dr. L. Lin for a critical reading of the manuscript.

Note added.—After this paper had been submitted for publication, the article by Barbero, G., and Meuti, M. (1986, *J. Phys., Paris*, **47**, 341) taking into account the influence of flexo-electricity was published. The situation investigated by Barbero and Meuti (that is a hybrid cell and without an applied field) is not identical to ours. For our case the flexo-electric effects are to be investigated in the future.

References

[1] Cognard, J., 1982, *Molec. Crystals liq. Crystals*, Suppl., **1**, 1.
[2] Derzhanski, A. I., and Hinov, H. P., 1983, *Molec. Crystals liq. Crystals*, **94**, 127.
[3] Barbero, G., Madhusudana, N. V., and Durand, G., 1984, *J. Phys. Lett., Paris*, **45**, L-613; 1984, *Z. Naturf.* (*a*), **39**, 1066.
[4] Sheng, P., 1975, *Introduction to Liquid Crystals*, edited by E. B. Priestley, P. J. Wojtowicz, and P. Sheng (Plenum Press), Chap. 8.

[5] De Gennes, P. G., 1974, *The Physics of Liquid Crystals* (Clarendon Press), Chap. 3.
[6] Nehring, J., Kmetz, A. R., and Scheffer, T. J., 1976, *J. appl. Phys.*, **47**, 850.
[7] Sprokel, G. J., Santo, R., and Swalen, J. D., 1981, *Molec. Crystals liq. Crystals*, **68**, 29.
[8] Yang, K. H., 1982, *J. appl. Phys.*, **53**, 6742.
[9] Mada, H., 1981, *Appl. Phys. Lett.*, **39**, 701.
[10] Mada, H., 1979, *Molec. Crystals liq. Crystals*, **51**, 43.
[11] Barbero, G., Bartolino, R., and Meuti, M., 1984, *J. Phys. Lett., Paris*, **45**, L-499.
[12] Nehring, J., and Saupe, A., 1971, *J. chem. Phys.*, **54**, 337.
[13] Faetti, S., and Palleschi, V., 1985, *J. Phys., Paris*, **46**, 415.
[14] Sprokel, G. J., 1981, *Molec. Crystals liq. Crystals*, **68**, 39. The notation in this paper is adopted here.
[15] Samsonov, G. V., 1982, *The Oxide Handbook*, 2nd edition (IFI/Plenum).
[16] K15 is 4-cyano-4′-*n*-pentylbiphenyl, and was obtained from BDH Chemicals Limited.
[17] Madhusudana, N. V., and Durand, G., 1985, *J. Phys. Lett., Paris*, **46**, L-195.